buildings

MDPI

Article

Experimental Study and Prediction of Strength and Stiffness Degradation of Boric-Acid-Corroded Concrete

Guodong Zhao [1], Xuan Zhang [2,3,*], Dafei Jiang [1] and Xinzhu Zhou [4]

[1] Engineering Management Department, CNNP Nuclear Power Operations Management Co., Ltd., Jiaxing 314300, China; zhaogd@cnnp.com.cn (G.Z.); jiangdf01@cnnp.com.cn (D.J.)
[2] Nuclear Power and Wind Power Division, MCC Inspection and Certification Co., Ltd., Beijing 100088, China
[3] State Key Laboratory of Coastal and Offshore Engineering, Dalian University of Technology, Dalian 116024, China
[4] College of Civil Engineering, Zhejiang University of Technology, Hangzhou 310032, China; xzzhou66@zjut.edu.cn
* Correspondence: zhangxuan1@cribc.com

Abstract

Durability tests were performed on concrete representative of nuclear power plant structures exposed to boric acid leakage. Boric acid is widely used in pressurized water reactor systems for neutron absorption and chemical control; therefore, accidental leakage or evaporation-induced concentration of borated water can create an important durability concern for adjacent concrete structures. Three boric acid concentrations (0, 2500 and 18,000 ppm) and two temperature levels (20 and 60 °C) were considered. The evolution of cube compressive strength and elastic modulus with exposure age was examined over 180 days. The results show a slight increase in concrete strength and stiffness during the early stage of exposure, followed by a continuous increase in the loss ratios of cube compressive strength and elastic modulus at later ages. The maximum measured strength–loss ratio was 4.684%, and the maximum measured elastic modulus–loss ratio was 1.755%. A service life prediction model based on loss ratio parameters was then developed from the test results. The fitted examples gave high coefficients of determination (R^2 = 0.9960 for cube compressive strength and R^2 = 0.9947 for elastic modulus), indicating that the proposed model can support durability assessment and aging management of boric-acid-corroded concrete structures in nuclear power plants.

Keywords: concrete; boric acid; cube compressive strength; elastic modulus; service-life prediction

Check for updates

Academic Editor: Mizan Ahmed

Received: 25 May 2026
Revised: 12 June 2026
Accepted: 15 June 2026
Published: 18 June 2026

Copyright: © 2026 by the authors. Licensee MDPI, Basel, Switzerland. This article is an open access article distributed under the terms and conditions of the Creative Commons Attribution (CC BY) license.

1. Introduction

Under normal service conditions in nuclear power plants, boric acid solution is weakly acidic, with a pH of approximately 4.8–5.2, and is separated from reinforced concrete structures by stainless steel pipes or liners. During abnormal leakage, however, evaporation can concentrate the solution. At 95 °C, saturated boric acid solution may have a pH below 3 and can therefore be highly corrosive. Because nuclear power plant buildings and structures are generally inspected and maintained only during outages, prolonged exposure of concrete members to boric acid may damage acid-soluble constituents in the cement paste and aggregates, thereby degrading concrete properties. Several boric acid leakage events have been reported worldwide. A systematic investigation of how boric acid corrosion affects concrete performance and service life is therefore important for managing the service life of concrete structures in nuclear power plants.

Boron-containing materials are also relevant to cement-based composites and durability engineering. Natural boron minerals such as colemanite have been investigated as mineral additions or functional constituents because their particle characteristics, calcium-bearing composition and borate chemistry may influence hydration, pore filling and resistance to aggressive environments. Recent work showed that raw ground colemanite substitution can improve concrete strength and durability under several exposure conditions [1], while nano-sized amorphous colemanite studies have clarified the morphology, crystal structure and thermal behavior of processed boron minerals [2]. These studies indicate that boron compounds can participate in material property development and corrosion resistance mechanisms, providing useful context for interpreting the response of concrete exposed to boric acid environments.

Agostini et al. [3] conducted accelerated leaching tests on hollow mortar cylinders and assessed leaching through elastic modulus, compressive strength, porosity and gas permeability. Their results showed that calcium leaching reduced mechanical performance and increased transport-related deterioration, with the leaching front developing approximately in proportion to the square root of exposure time. Nguyen et al. [4] used a 6 mol/L ammonium nitrate solution to accelerate the leaching of cylindrical concrete specimens and measured the associated mechanical degradation. Both studies showed that leaching reduces the strength and stiffness of cementitious materials while increasing ductility, porosity and permeability. Ramm and Biscoping [5] investigated the effect of boric acid on cracked reinforced concrete members. Their results showed that the initial aggressiveness of boric acid depends on solution pH; lower pH values produce more pronounced corrosion, although the resulting reduction in member cross-section may be limited.

Jin et al. [6,7] and Zhan et al. [8] examined the durability of reinforced concrete in boric acid environments. At the macroscopic level, these studies found that boric acid has limited corrosive effects on concrete and steel and does not markedly impair the service performance of reinforcement or concrete. At the microscopic level, the main reaction product between boric acid (H_3BO_3) and cement paste was identified as calcium metaborate, $Ca(BO_2)_2$; this alkaline product, with a pH above 11, may slow further corrosion. X-ray diffraction indicated that boric acid attack was largely confined to the concrete surface. Wang et al. [9] and Jiang [10] evaluated reinforced concrete after boric acid exposure and concluded that the corrosion effect is relatively weak and concentration-dependent. Wang et al. [11] further reported that concrete exposed to 20 and 40 °C boric acid environments remained relatively stable, whereas a very high concentration of 180,000 ppm at 70 °C reduced compressive strength by 27.8% and caused severe surface corrosion and harmful-pore development. Le [12] and Jiang et al. [13] exposed concrete to boric acid environments and conducted mechanical tests. They reported that the loss ratio of mechanical properties increased with exposure time, whereas boric acid concentration had no obvious effect on either the magnitude or the growth rate of the loss ratio. For service life prediction, Le [12] considered the actual service life to remain equal to the design service life. Rong et al. [14] extracted cores from a leaking boric acid water tank at a nuclear power plant in China and performed macro- and micro-scale tests. The precipitates on the corroded core surfaces were highly crystalline borates, mainly calcium metaborate; the compressive strength of cores from the corroded area was slightly lower than that of uncorroded cores but still exceeded the standard concrete compressive strength of 30 MPa.

Previous studies have therefore established that boric acid attack is often surface-dominated and may be relatively mild at moderate concentration and temperature, but they also show that degradation becomes more significant under high concentration, high temperature and long exposure. Recent research on the long-term performance of steel–concrete composite wall panels has also emphasized the importance of realistic

engineering boundary conditions and sustained service actions in structural performance assessment [15]. However, quantitative evidence remains limited for the coupled effects of boric acid concentration and temperature on both strength and stiffness of nuclear power plant concrete over long exposure durations. The specific contribution of this study is threefold: (i) concrete representative of nuclear power plant structures was tested; (ii) boric acid concentration and temperature were considered simultaneously over a 180-day exposure program; and (iii) a loss-ratio-based service life prediction model was established for both cube compressive strength and elastic modulus. The findings support durability assessment and performance improvement of concrete structures exposed to boric acid.

2. Materials and Methods

2.1. Materials

Concrete specimens were cast using a typical nuclear power plant concrete mixture, as shown in Table 1. The water-to-binder ratio of 0.35 was selected to represent dense structural concrete used in nuclear power plant engineering, where low permeability and reliable mechanical performance are required. Class I fly ash was incorporated to improve workability, refine pore structure and enhance long-term durability. After casting, the specimens were kept in a dry-curing room for 2 days before demolding. They were then cured for 28 days in a standard curing room at 20 ± 0.5 °C and 100% relative humidity, after which their mass and compressive strength were measured.

Table 1. Mix proportion of concrete.

Water/Binder Ratio	Cement (kg/m^3)	Fly Ash (kg/m^3)	Water (kg/m^3)	Medium Sand (kg/m^3)	Crushed Stone 1 (kg/m^3)	Crushed Stone 2 (kg/m^3)	Pumping Agent (kg/m^3)
0.35	354.6	88.6	155.3	743.6	395.7	609.4	4.4

Note: the particle size of crushed stone 1 was 4.75–9.5 mm, and that of crushed stone 2 was 9.5–20 mm. The dosage of pumping agent was 1% of the binder mass. Aggregates were in saturated surface-dry condition during mixing.

P·O 42.5 ordinary Portland cement (Zhejiang Qianchao Cement Factory, Hangzhou, China) was used; its chemical composition and physical–mechanical properties are listed in Tables 2 and 3, respectively. Class I fly ash was used, and its chemical composition is shown in Table 4. Natural river sand served as the fine aggregate, with a mud content of 1.54%, apparent density of 2630 kg/m^3, moisture content of 0.35% and water absorption of 1.41%. Crushed stone served as the coarse aggregate, with an apparent density of 2530 kg/m^3, moisture content of 0.35% and water absorption of 1.13%. Municipal tap water with pH = 7.4 ± 0.5 was used for both mixing and curing. A ZWL-A-II high-efficiency pumping agent was added at 1% of the binder mass; its performance indicators are listed in Table 5. The relatively low water content was therefore achieved with the aid of this pumping agent, which provided the required workability and compaction performance.

Table 2. Chemical composition of cement [16].

Component	SiO_2	Al_2O_3	Fe_2O_3	CaO	MgO	SO_3	Loss
Content (%)	21.24	5.95	3.15	61.43	3.78	2.22	2.21

Table 3. Physical and mechanical properties of cement [16].

Initial Setting Time (min)	Final Setting Time (min)	Flexural Strength, 3 d (MPa)	Flexural Strength, 28 d (MPa)	Compressive Strength, 3 d (MPa)	Compressive Strength, 28 d (MPa)
186	325	5.0	8.2	21.2	48.3

Table 4. Main chemical composition of fly ash [16].

Component	SiO_2	Al_2O_3	CaO	Fe_2O_3	SO_3	TiO_2	K_2O	MgO
Content (%)	51.25	30.47	6.48	4.66	1.55	1.19	0.97	0.66

Table 5. Performance indicators of the pumping agent.

Item	pH	Chloride Ion Content (%)	Density (g/cm^3)	Solid Content (%)	Total Alkali Content (%)	Water Reduction Rate of Mortar (%)
Requirement	≥6.0	≤1.0	1.23 ± 0.03	38.0 ± 1.9	≤8.0	≥17
Test result	9.3	0.07	1.219	37.52	5.11	Qualified

Boric acid (H_3BO_3) produced in Chile was used to prepare the corrosion solutions. The boric acid had a purity greater than 99.9%, appeared as pure white crystals and was stored in sealed drums before use. For concentration monitoring, a 1% phenolphthalein standard indicator solution with a pH transition range of 8.2–10.0 was used. Mannitol supplied by Zhejiang Bokun Biotechnology Co., Ltd. (Ningbo, China) was used to enhance titration of boric acid in the sampled solutions. Analytical-grade hydrochloric acid and sodium hydroxide standard titration solutions, both with a concentration of 0.1 mol/L, were used during solution analysis.

2.2. Test Methods and Experimental Design

Boric acid solutions with concentrations of 2500 ppm and 18,000 ppm were prepared, with a 0 ppm group serving as the control. The 2500 ppm solution represented the condition of a nuclear power plant refueling water pool, whereas the 18,000 ppm solution was used for accelerated corrosion. This higher concentration was selected to represent the concentration increase that may occur after leakage and evaporation of borated water, and to obtain measurable degradation within a practical laboratory duration. To keep the boric acid concentration within the target range, solution samples were taken periodically from the test boxes and analyzed through titration. Mannitol was added to strengthen the titration response of boric acid, phenolphthalein was used as the indicator, and the solution was titrated with the NaOH solution to determine the boric acid concentration. When the measured concentration was outside the preset range, the solution was replaced by pumping out the waste liquid and adding freshly prepared boric acid solution. The 0 ppm group served as the blank control and did not require solution replacement.

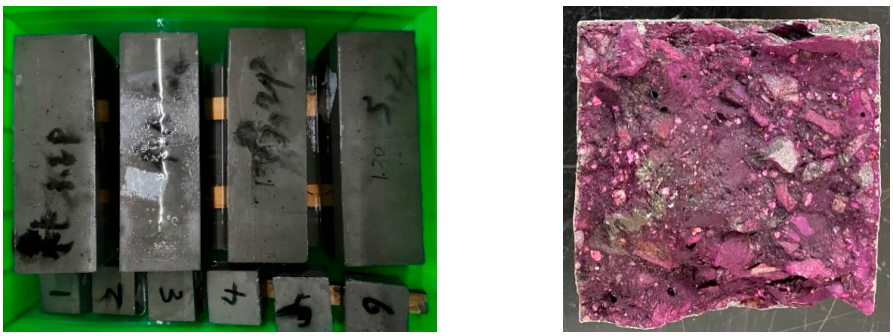
Two temperatures were used: 20.0 °C, representing normal temperature, and 60.0 °C, representing elevated temperature. The 60 °C condition was selected as an accelerated and engineering-relevant temperature level for local high-temperature leakage, evaporation or accident-related exposure scenarios in nuclear power plant facilities. The normal temperature tests were conducted in a curing room at 20.0 ± 2.0 °C and at least 95% relative humidity, whereas the elevated temperature tests were conducted in a multifunctional climate simulation chamber.

The specimens were divided into six groups according to the study objectives (Table 6). For each group and testing age, the mean value of three specimens was used as the measured result. Cubes measuring 100 mm × 100 mm × 100 mm were used for compressive strength testing, and prisms measuring 100 mm × 100 mm × 300 mm were used for elastic modulus testing.

Table 6. Experimental groups.

Temperature (°C)	Boric Acid Concentration (ppm)	Group
20	0	C23(1)
20	2500	C23(2)
20	18,000	C23(3)
60	0	C63(1)
60	2500	C63(2)
60	18,000	C63(3)

After 28 days of standard curing, the specimens were fully immersed in boric acid solution; the immersion environment and specimen morphology after 180 days of immersion are shown in Figure 1. Measurements were taken every 30 days over a total exposure period of 180 days. Wooden spacers were placed between specimens to ensure sufficient contact with the solution and to reduce errors caused by incomplete exposure, and the test box was covered with curing film. To reduce the influence of moisture content differences on the measured mechanical properties, the specimens were also cured through full immersion during the 28-day standard curing period.



(**a**) (**b**)

Figure 1. Specimen immersion environment and morphology after 180 days of immersion. (**a**) Immersion environment; (**b**) phenolphthalein-stained surface morphology of concrete cubes after 180 days.

2.3. Cube Compressive Strength

To quantify the effect of boric acid attack on concrete compressive strength, cube compressive strength was measured periodically. The extent of corrosion under different exposure conditions was characterized by the cube compressive strength–loss ratio.

The cube compressive strength–loss ratio of concrete was calculated as follows:

$$d_c = \frac{f_{cn} - f_{cb}}{f_{cn}} \times 100\% \quad (1)$$

where d_c is the cube compressive strength–loss ratio of concrete (%); f_{cb} is the cube compressive strength of concrete immersed in boric acid solution (MPa); and f_{cn} is the cube compressive strength of concrete immersed in natural curing water (MPa).

Cube compressive strength was determined according to Standard for Test Methods of Concrete Physical and Mechanical Properties (GB/T 50081-2019 [17]). The testing machine was an STYE-3000C compression testing machine manufactured by Zhejiang Tugong Instrument Co., Ltd. (Shaoxing, China). The loading rate was 0.50 MPa/s, and the correction coefficient was 0.95.

2.4. Elastic Modulus

To quantify the effect of boric acid attack on concrete stiffness, the elastic modulus was measured periodically. The extent of corrosion under different exposure conditions was characterized by the elastic modulus–loss ratio.

The elastic modulus–loss ratio of boric-acid-corroded concrete was defined as follows:

$$d_e = \frac{E_n - E_b}{E_n} \times 100\% \quad (2)$$

where d_e is the elastic modulus–loss ratio of the specimen (%); E_b is the elastic modulus of concrete immersed in boric acid solution (GPa); and E_n is the elastic modulus of concrete immersed in natural curing water (GPa).

Elastic modulus was measured according to GB/T 50081-2019. The testing machine was a WAW-1000 closed-loop electro-hydraulic servo testing machine (Changchun Testing Machine Co., Ltd., Changchun, China). The elastic modulus test setup is shown in Figure 2.



Figure 2. Elastic modulus test of concrete.

3. Results and Discussion

3.1. Cube Compressive Strength

Table 7 shows the experimental results of cube compressive strength, and Table 8 and Figure 3 show the time-dependent evolution of the cube compressive strength–loss ratio. During the first 1–3 months of immersion, the loss ratio was negative. After 3 months, it increased with exposure time. This early behavior is attributed to the reaction between boric acid (H_3BO_3) and calcium hydroxide, $Ca(OH)_2$, in the pore solution near the specimen surface, which forms calcium metaborate crystals, $Ca(BO_2)_2$, that may block pores. The dense concrete matrix also hindered penetration of the acidic medium, while the alkalinity of concrete provided a buffering effect. Together, these effects gave the concrete some resistance to the acidic environment and slowed the corrosion process. This interpretation is consistent with previous XRD/SEM observations in which calcium borate products were detected near the concrete surface after boric acid exposure [7,11]. However, because no direct microstructural tests were conducted in the present study, the pore-blocking mechanism should be regarded as an inference supported by previous studies rather than direct evidence from the present specimens.

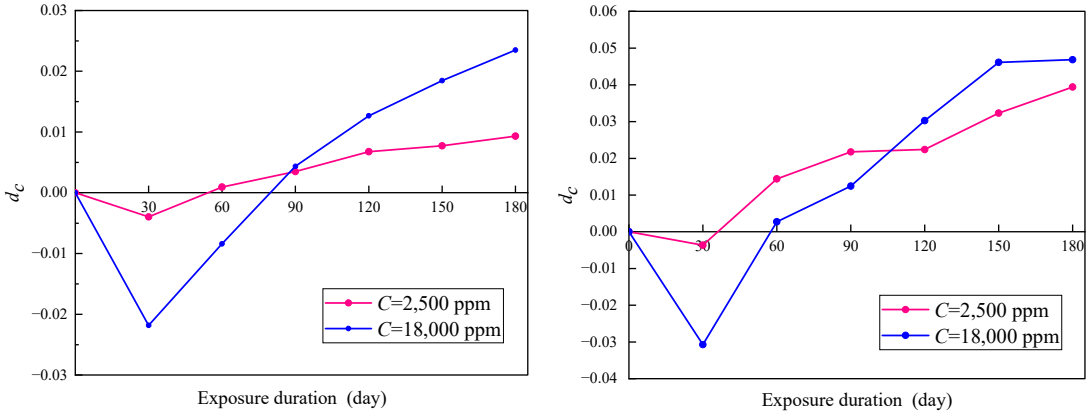


Figure 3. Cube compressive strength–loss ratio of concrete specimens immersed in boric acid solution. (**a**) T = 20 °C; (**b**) T = 60 °C.

Table 7. Experimental results of cube compressive strength (MPa).

Exposure Duration (Day)	C23(1)	C23(2)	C23(3)	C63(1)	C63(2)	C63(3)
0	45.80	45.80	45.80	45.80	45.80	45.80
30	50.40	50.60	51.50	60.25	60.47	62.10
60	53.50	53.45	53.95	62.40	61.50	62.23
90	57.60	57.40	57.35	64.40	63.00	63.60
120	59.20	58.80	58.45	66.08	64.60	64.08
150	59.60	59.14	58.50	67.20	65.03	64.10
180	60.05	59.49	58.64	67.25	64.60	64.10

Table 8. Experimental results of cube compressive strength–loss ratio (%).

Exposure Duration (Day)	C23(2)	C23(3)	C63(2)	C63(3)
0	0	0	0	0
30	−0.397	−2.183	−0.365	−3.071
60	0.093	−0.841	1.442	0.272
90	0.347	0.434	2.174	1.242
120	0.676	1.267	2.240	3.027
150	0.772	1.846	3.229	4.613
180	0.933	2.348	3.941	4.684

Compared with the literature, the moderate deterioration observed in this study is consistent with studies reporting weak or surface-limited boric acid attack at concentrations of 2000–30,000 ppm [6–9]. It is also consistent with Wang et al. [11], who reported stable performance at 20 and 40 °C for moderate boric acid concentrations but severe deterioration under the much harsher condition of 180,000 ppm and 70 °C. The present 18,000 ppm and 60 °C condition therefore occupies an intermediate accelerated exposure range and provides useful data for service life prediction without reaching the extreme deterioration level reported for very high boric acid concentration. In addition, studies on boron-containing ceramic reinforcement in metal composites have shown that boron carbide (B_4C) additions can affect corrosion kinetics and corrosion resistance, supporting the broader interpretation that boron-bearing phases may influence degradation processes in aggressive environments [18].

At the same temperature, higher boric acid concentration produced a higher cube compressive strength–loss ratio. The 18,000 ppm groups consistently showed greater loss ratios than the 2500 ppm groups. This is partly because increasing boric acid concentration lowers the solution pH, thereby accelerating corrosion, and partly because a higher concentration promotes faster boric acid diffusion into the concrete.

At the same boric acid concentration, higher temperature also increased the cube compressive strength–loss ratio. During the early stage, elevated temperature accelerated cement hydration and promoted the formation of hydration products, leading to faster strength development. It also promoted reactions between the boric acid solution and hydration products, generating slightly soluble calcium metaborate crystals that blocked pores and delayed further attack. As a result, at 60 °C, both the rate of strength gain and the absolute value of the negative loss ratio were higher than at 20 °C. After 60 days, boric acid attack became dominant as hydration weakened. Elevated temperature increased ion diffusivity and continued to accelerate reactions between boric acid and concrete. Boric acid then reacted with the cement paste, damaging the solid phase and increasing deleterious pores within the specimens. Elevated temperature could also induce microcracking and aggregate debonding. The temperature effect should therefore be interpreted as the combined result of temperature-induced hydration, possible thermal damage and chemical corrosion. Because the 60 °C control group may also experience temperature-related changes unrelated to boric acid attack, the control group data should be explicitly reported and discussed when interpreting the boric acid loss ratios.

3.2. Elastic Modulus

Table 9 shows the experimental results of elastic modulus. Table 10 and Figure 4 show the time-dependent evolution of elastic modulus–loss ratio. During the early immersion stage, the elastic modulus–loss ratio differed slightly from the strength–loss ratio. Negative elastic modulus–loss ratios were not observed in the two groups tested at 60 °C, whereas both groups tested at 20 °C showed negative values. After 3 months of immersion, the elastic modulus–loss ratio increased with exposure time, although it remained generally lower than the strength–loss ratio. Boric acid concentration had a pronounced effect on elastic modulus, and this effect became more evident at higher temperature. The temperature effect on elastic modulus–loss, however, differed from its effect on strength loss.

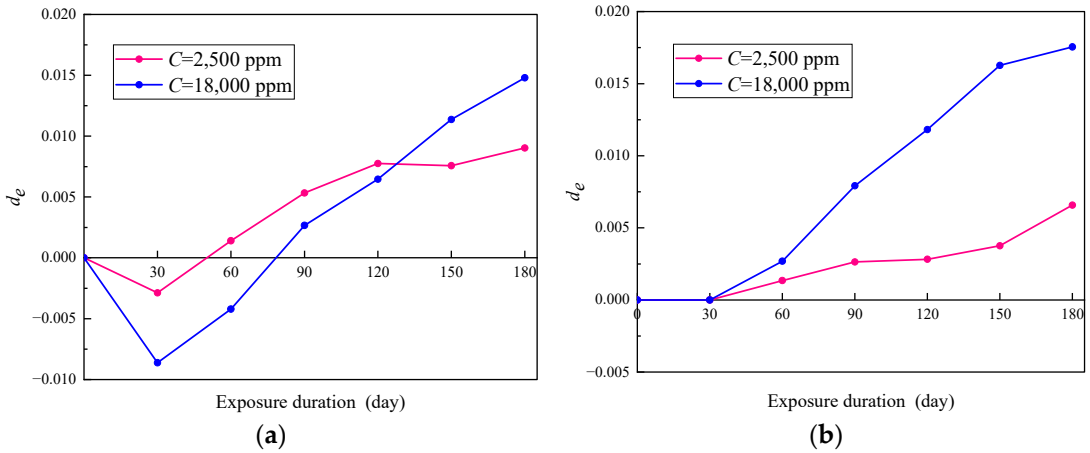


Figure 4. Elastic modulus–loss ratio of concrete specimens immersed in boric acid solution. (**a**) T = 20 °C; (**b**) T = 60 °C.

Table 9. Experimental results of elastic modulus (GPa).

Exposure Duration (Day)	C23(1)	C23(2)	C23(3)	C63(1)	C63(2)	C63(3)
0	34.60	34.60	34.60	34.55	34.55	34.55
30	34.80	34.90	35.10	36.75	36.75	36.75
60	35.60	35.55	35.75	37.20	37.15	37.10
90	37.50	37.30	37.40	37.90	37.80	37.60
120	38.70	38.40	38.45	38.91	38.80	38.45
150	39.60	39.30	39.15	39.95	39.80	39.30
180	39.88	39.52	39.29	41.02	40.75	40.30

Table 10. Experimental results of elastic modulus–loss ratio (%).

Exposure Duration (Day)	C23(2)	C23(3)	C63(2)	C63(3)
0	0	0	0	0
30	−0.287	−0.862	0.000	0.000
60	0.140	−0.421	0.134	0.269
90	0.533	0.267	0.264	0.792
120	0.775	0.646	0.283	1.182
150	0.758	1.136	0.375	1.627
180	0.903	1.479	0.658	1.755

During the first 1–3 months of immersion, exposure to boric acid solution was more favorable to strength and stiffness development than curing in natural water. After 3 months, however, both strength and stiffness loss ratios increased with exposure time. In the early stage, the small amount of calcium metaborate produced by the reaction filled pores and improved strength and stiffness; this filling effect became more pronounced at higher concentration. Continued cement hydration also increased the amount of calcium hydroxide, further supporting strength and stiffness development. In the later stage, calcium metaborate increased substantially while calcium hydroxide decreased, adversely affecting concrete strength and stiffness. Similar two-stage behavior has been reported in boric-acid-corroded concrete, where early pore filling and continued hydration can temporarily offset deterioration, followed by progressive degradation as exposure continues [11,19]. In the present study, the maximum elastic modulus–loss ratio was 1.755%, which was lower than the maximum cube compressive strength–loss ratio of 4.684%, indicating that stiffness degraded more slowly than strength under the tested boric acid exposure conditions.

4. Prediction Model for Loss Ratio in a Boric-Acid Environment

Based on the degradation characteristics of cube compressive strength and elastic modulus under boric acid attack, a total damage rate model was developed to predict the service life of reinforced concrete after boric acid corrosion. The model follows an empirical damage evolution form used in durability and service life prediction, in which damage growth is described as a time-dependent function calibrated from measured deterioration indicators [12,16,19]. The model is expressed as follows:

$$D_t = \frac{1}{1 + a\, t^b} \tag{3}$$

where D_t is the total damage rate of concrete at time. $D_t = 0$ indicates no loss of concrete performance, whereas $D_t = D_f$ indicates durability failure of the concrete structure, where D_f is the prescribed durability failure–loss ratio. Parameters a and b are fitting coefficients. Parameter a controls the magnitude or scale of the damage development curve, whereas parameter b controls the curvature and rate of time-dependent deterioration. These parameters should therefore be interpreted as empirical indicators of corrosion severity under each exposure condition rather than as directly measured material constants.

Because negative loss ratios occurred during the early stage for both cube compressive strength and elastic modulus, the coordinate axes were shifted to avoid bias in service life prediction. Equation (3) was therefore modified as follows:

$$D'_t = \frac{1 - D_i}{1 + a\, t'^b} \tag{4}$$

$$t' = t - t_i, \quad D'_t = D_t - D_i \tag{5}$$

where t_i is the exposure age corresponding to a measured loss ratio of zero (d), and D_i is the minimum measured loss ratio in the concrete tests ($D_i < 0$).

4.1. Service Life Prediction Model Based on Cube Compressive Strength–Loss Ratio

For a prescribed cube compressive strength–loss ratio D_w, the shifted target loss ratio is $D'_w = D_w - D_i$. When $D'_t = D'_w$, the cube compressive strength–loss ratio reaches the prescribed value. The fitting parameters a and b can then be determined, and the concrete service life t can be obtained by inverting Equation (4):

$$t = t_i + \left[\frac{1 - D_i}{a(D_w - D_i)}\right]^{1/b} \tag{6}$$

Taking the cube compressive strength–loss ratio of the test group at 20 °C and 2500 ppm boric acid concentration as an example, Equation (4) was used to calculate parameters a and b, as shown in Equation (7). The resulting trend of the cube compressive strength–loss ratio under this condition is shown in Figure 5. The coefficient of determination R^2 was 0.9960, indicating good agreement between experimental and calculated values. Therefore, the model can be used to predict the cube compressive strength–loss ratio of concrete in a boric acid environment.

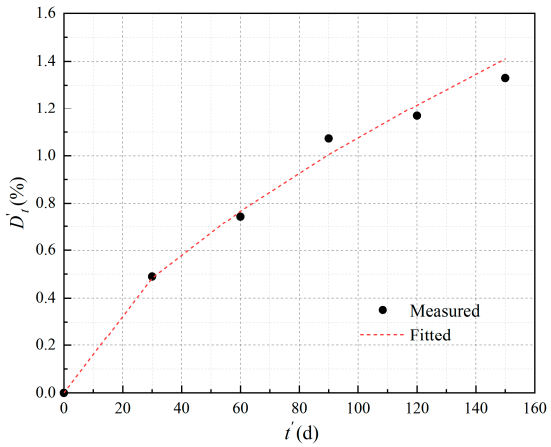


Figure 5. Fitted curve of the cube compressive strength–loss ratio for the C23(2) group.

Because the same experimental data set was used for calibration and goodness-of-fit evaluation, the predictive capability of the model remains subject to uncertainty. Compared with the earlier approach by Le [12], which treated the actual service life as remaining

equal to the design service life under limited observed deterioration, the present model provides threshold-dependent service life estimates based on measured loss ratios. Recent boric acid concrete studies have further linked performance degradation with macro- and microstructural changes and have used empirical modeling to describe time-dependent deterioration in nuclear power plant exposure scenarios [16,19]. The present model is consistent with these studies in using mechanical performance loss as the degradation indicator, but it separately calibrates strength- and stiffness-based damage curves for each concentration–temperature condition. This improves comparability between exposure groups, while also showing that the fitted coefficients should be understood as empirical indicators within the tested range rather than universal material constants.

$$D'_{t'} = \frac{1-(-0.00397)}{1+2025.2t'^{-0.671}} \quad (7)$$

Measured and fitted $D'_{t'}$ based on cube compressive strength–loss ratio are summarized in Table 11.

Table 11. Measured and fitted $D'_{t'}$ based on cube compressive strength–loss ratio (%).

t' (d)	Measured	Fitted
0 (t = 30)	0.000	0.000
30 (t = 60)	0.490	0.483
60 (t = 90)	0.744	0.767
90 (t = 120)	1.073	1.005
120 (t = 150)	1.169	1.216
150 (t = 180)	1.330	1.410

Fitted parameters based on cube compressive strength–loss ratio for each group are shown in Table 12. The values D_f = 5%, 10%, 15%, 20% and 25% were selected and substituted into Equation (6) to calculate the service life of concrete corresponding to different loss ratios. The predicted service lives of the concrete specimens in each group are shown in Table 13 and Figure 6.

Table 12. Fitted parameters based on cube compressive strength–loss ratio.

Group	D_i	a	b	R^2
C23(2)	−0.397%	2025.2	−0.671	0.9960
C23(3)	−0.841%	720.1	−0.662	0.9982
C63(2)	−0.365%	258.5	−0.460	0.9685
C63(3)	−3.071%	144.9	−0.479	0.9652

Table 13. Predicted service life based on cube compressive strength–loss ratio (y).

D_E	C23(2)	C23(3)	C63(2)	C63(3)
5%	3.311	1.005	1.013	0.599
10%	9.381	2.485	4.463	1.666
15%	18.262	4.651	11.754	3.592
20%	30.340	7.605	24.650	6.715
25%	46.268	11.515	45.642	11.514

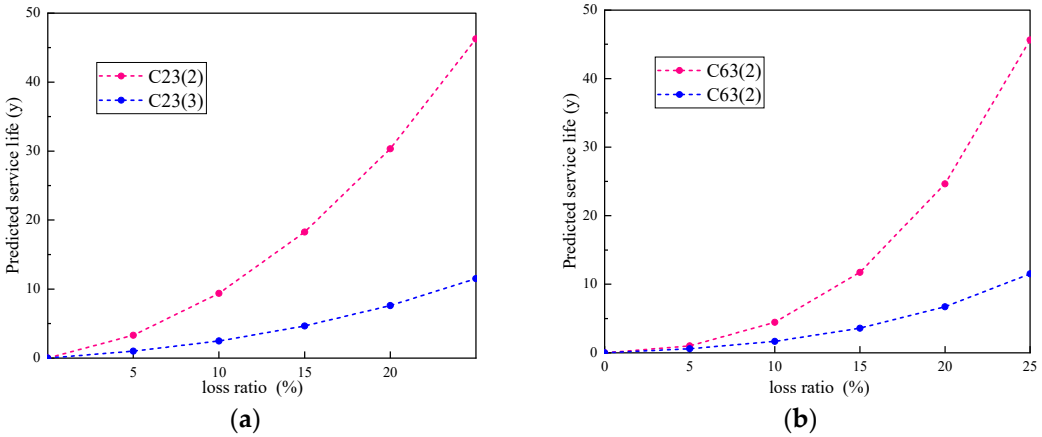


Figure 6. Predicted service life of concrete specimens based on cube compressive strength–loss ratio. (**a**) T = 20 °C; (**b**) T = 60 °C.

At a given temperature, the predicted service life of concrete decreased markedly as boric acid concentration increased. At the same boric acid concentration, the predicted service life at 60 °C was shorter than that at 20 °C. For all groups, a higher failure threshold for cube compressive strength–loss corresponded to a longer predicted service life.

4.2. Service Life Prediction Model Based on Elastic Modulus–Loss Ratio

Taking the elastic modulus–loss ratio of the group tested at 20 °C and 18,000 ppm boric acid concentration as an example, Equation (4) was used to calculate the fitting parameters a and b, as shown in Equation (8). The variation trend of the elastic modulus–loss ratio under this condition is shown in Figure 7. The coefficient of determination R^2 was 0.9947, indicating good agreement between measured and calculated elastic modulus–loss ratios. Therefore, the model can be used to predict the elastic modulus–loss ratio of concrete in a boric acid environment.

$$D'_{t'} = \frac{1-(-0.00862)}{1+2272.4t'^{-0.795}} \quad (8)$$

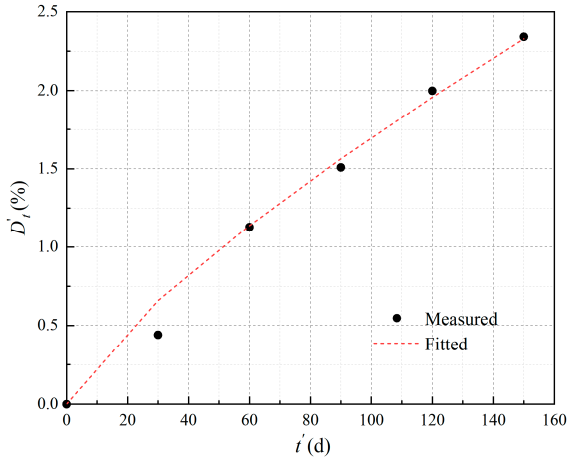


Figure 7. Fitted curve of the elastic modulus–loss ratio for the C23(3) group.

Measured and fitted $D'_{t'}$ based on elastic modulus–loss ratio are summarized in Table 14.

Table 14. Measured and fitted $D'_{t'}$ based on elastic modulus–loss ratio (%).

t' (d)	Measured	Fitted
0 (t = 30)	0.000	0.000
30 (t = 60)	0.441	0.659
60 (t = 90)	1.129	1.137
90 (t = 120)	1.508	1.563
120 (t = 150)	1.998	1.957
150 (t = 180)	2.341	2.329

Fitted parameters based on elastic modulus–loss ratio for each group are shown in Table 15.

Table 15. Fitted parameters based on elastic modulus–loss ratio.

Group	D_i	a	b	R^2
C23(2)	−0.287%	2243.3	−0.683	0.9765
C23(3)	−0.862%	2272.4	−0.795	0.9947
C63(2)	0	15,945	−0.886	0.9767
C63(3)	0	6041.8	−0.913	0.9487

The values D_E = 5%, 10%, 15%, 20% and 25% were selected and substituted into Equation (6) to calculate the concrete service life corresponding to each loss ratio. The service lives of the concrete specimens in each group are shown in Table 16 and Figure 8.

Table 16. Predicted service life based on elastic modulus–loss ratio (y).

D_E	C23(2)	C23(3)	C63(2)	C63(3)
5%	3.297	1.457	5.467	1.509
10%	9.302	3.278	12.707	3.420
15%	17.986	5.611	21.420	5.676
20%	29.691	8.505	31.736	8.313
25%	45.012	12.051	43.910	11.392

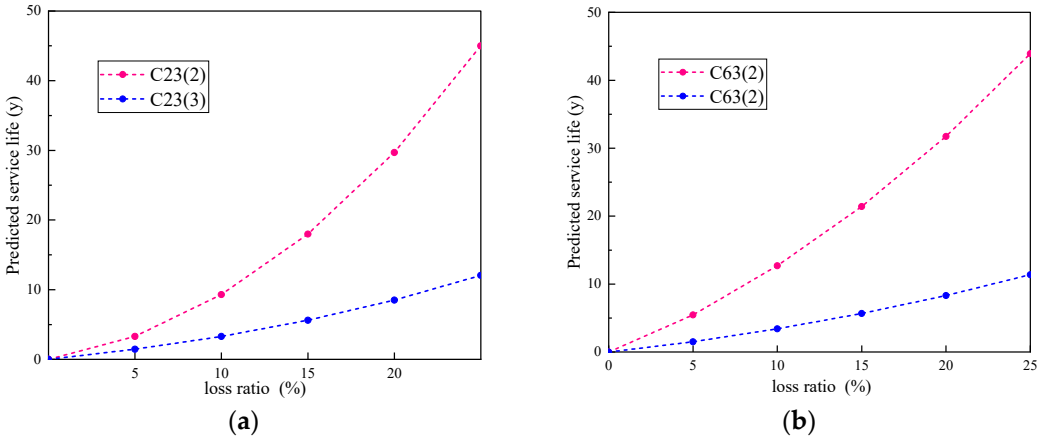


Figure 8. Predicted service life of concrete specimens based on elastic modulus–loss ratio. (**a**) T = 20 °C; (**b**) T = 60 °C.

The predicted service life of concrete decreased as boric acid concentration and temperature increased. Under the same test conditions and loss ratio thresholds, the service life predicted from elastic modulus was slightly longer than that predicted from cube compressive strength. This is consistent with the experimental observation that the elastic modulus–loss ratio was lower than the cube compressive strength–loss ratio, indicating that stiffness degraded more slowly than strength under boric acid attack.

Tables 12 and 15 summarize the fitted parameters and coefficients of determination for all exposure groups, while Tables 13 and 16 summarize the predicted service lives. These tables allow readers to verify the calculations and compare the effects of boric acid concentration and temperature more clearly.

5. Conclusions

This study conducted durability tests on concrete exposed to simulated boric acid environments. The effects of boric acid concentration and temperature on the degradation of cube compressive strength and elastic modulus were evaluated, and service life prediction models were established based on the corresponding loss ratios. The main conclusions are as follows:

(1) During the first 1–3 months of immersion, boric acid solution was more favorable than natural curing water for the development of concrete strength and stiffness. After 3 months, the loss ratios of both strength and stiffness increased with boric acid exposure time.

(2) Boric acid concentration strongly affected the strength and stiffness of boric-acid-corroded concrete. Increasing concentration markedly increased both the cube compressive strength–loss ratio and the elastic modulus–loss ratio.

(3) Temperature also affected the corrosion rate of concrete exposed to boric acid. Overall, the 60 °C groups showed slightly faster degradation and a slightly shorter predicted service life than the 20 °C groups.

(4) A total damage rate model was proposed. Its predictions agreed well with the experimental data and can be used as a reference for service life prediction of reinforced concrete subjected to boric acid corrosion. The model parameters should be further validated with independent data before direct engineering application.

The results provide an experimental basis for evaluating boric acid leakage effects in nuclear power plant concrete structures. In engineering practice, the proposed loss ratio approach can support aging management, inspection planning, maintenance prioritization and preliminary service life assessment after suspected boric acid exposure. Future studies should expand the sample size, report statistical variability, include additional boric acid concentrations and temperature levels, and combine mechanical testing with SEM, XRD, MIP, TG/DSC or other microstructural observations. Long-term field data should also be used to validate and refine the proposed prediction model.

Author Contributions: Conceptualization, G.Z.; methodology, D.J.; validation, G.Z.; investigation, G.Z. and X.Z. (Xuan Zhang); resources, X.Z. (Xinzhu Zhou); data curation, X.Z. (Xinzhu Zhou); writing—original draft preparation, X.Z. (Xuan Zhang); writing—review and editing, X.Z. (Xuan Zhang) and X.Z. (Xinzhu Zhou); visualization, D.J.; supervision, D.J.; funding acquisition, D.J. All authors have read and agreed to the published version of the manuscript.

Funding: This research was funded by the Scientific Research Project of CNNP Nuclear Power Operations Management Co., Ltd. (No. Y-2021-0141) and the National Science Foundation for Excellent Young Scholars of China (No. 52222808).

Data Availability Statement: The data are not publicly available due to institutional and project restrictions. The data may be available from the corresponding author upon reasonable request and with permission from the relevant institution.

Conflicts of Interest: Xuan Zhang is employed by Nuclear Power and Wind Power Division, MCC Inspection and Certification Co., Ltd., and Guodong Zhao and Dafei Jiang are employed by the Engineering Management Department, CNNP Nuclear Power Operations Management Co., Ltd. The remaining authors declare that the research was conducted in the absence of any commercial or financial relationships that could be construed as a potential conflict of interest.

References

1. Kara, C.; Kütük, S.; Kütük-Sert, T. Improvement of the durability of concrete by substitution of raw ground colemanite. *Case Stud. Constr. Mater.* **2023**, *19*, e02393. [CrossRef]
2. Kütük, S. Morphology, crystal structure and thermal properties of nano-sized amorphous colemanite synthesis. *Arab. J. Sci. Eng.* **2024**, *49*, 11699–11716. [CrossRef]
3. Agostini, F.; Lafhaj, Z.; Skoczylas, F.; Loodsveldt, H. Experimental study of accelerated leaching on hollow cylinders of mortar. *Cem. Concr. Res.* **2007**, *37*, 71–78. [CrossRef]
4. Nguyen, V.H.; Colina, H.; Torrenti, J.M.; Boulay, C.; Nedjar, B. Chemo-mechanical coupling behaviour of leached concrete: Part I: Experimental results. *Nucl. Eng. Des.* **2007**, *237*, 2083–2089. [CrossRef]
5. Ramm, W.; Biscoping, M. Autogenous healing and reinforcement corrosion of water-penetrated separation cracks in reinforced concrete. *Nucl. Eng. Des.* **1998**, *179*, 191–200. [CrossRef]
6. Jin, X.Y.; Jin, N.G.; Tian, Y. Study on the behavior and durability of reinforced concrete in boric acid environment. *Key Eng. Mater.* **2009**, *400–402*, 441–446. [CrossRef]
7. Jin, H.Z.; Li, Q.; Jin, X.Y.; Tian, Y.; Jin, N.G. Microstructure and durability of reinforced concrete in boric acid. *Adv. Mater. Res.* **2011**, *250–253*, 252–256. [CrossRef]
8. Zhan, Y.; Li, Q.; Jin, X.Y.; Tian, Y.; Jin, N.G. Behavior of reinforced concrete subjected to boric acid corrosion of nuclear power plant. *Adv. Mater. Res.* **2011**, *250–253*, 242–246. [CrossRef]
9. Wang, Q.Y.; Zhang, J.G.; Shan, M.C.; Yu, B.Y.; Zhao, Y.; Yang, R. Experimental study on the effect of boric acid corrosion on the performance of reinforced concrete. *Adv. Mater. Sci. Eng.* **2021**, *2021*, 5534917. [CrossRef]
10. Jiang, H.D. Experimental Study on the Influence of Boric acid Corrosion on the Performance of Reinforced Concrete in Nuclear Power Plants. Master's Thesis, Qingdao University of Technology, Qingdao, China, 2019. (In Chinese)
11. Wang, Y.; Huang, B.; Mao, Z.; Deng, M.; Cao, H. Effect of a boric acid corrosive environment on the microstructure and properties of concrete. *Materials* **2020**, *13*, 5036. [CrossRef] [PubMed]
12. Le, J.F. Experimental Study and Life Prediction of Reinforced Concrete Corroded by Boric Acid. Master's Thesis, Zhejiang University, Hangzhou, China, 2005. (In Chinese)
13. Jiang, H.D.; Zhang, J.G.; Sun, J.; Wang, P.; Wang, Q. Experimental study on the effect of boric acid corrosion on the mechanical properties of reinforced concrete. *J. Qingdao Univ. Technol.* **2019**, *40*, 16–22. (In Chinese)
14. Rong, H.; Yang, L.; Li, J.W.; Wang, Y. Durability of concrete structures in a nuclear power plant with boric-acid leakage. *Ind. Constr.* **2017**, *47*, 35–38. (In Chinese) [CrossRef]
15. Wang, Y.; Khan, M.; Uy, B.; Katwal, U.; Tao, Z.; Thai, H.-T.; Ngo, T. Long-term performance of steel-concrete composite wall panels under axial compression. *Structures* **2024**, *64*, 106606. [CrossRef]
16. Rong, H.; Geng, Y.; Tao, J.; Zhou, X.; Zheng, J.; Jia, Y. Experiment and modelling of performance degradation of boric acid-corroded concrete in nuclear power plants. *Case Stud. Constr. Mater.* **2025**, *23*, e04932. [CrossRef]
17. *GB/T 50081-2019*; Standard for Test Methods of Mechanical Properties of Concrete. China Architecture & Building Press: Beijing, China, 2019.
18. Çelebi, M.; Çanakçı, A.; Kütük, S. Influence of nano-sized ceramic reinforcement content on the powder characteristics and the mechanical, tribological, and corrosion properties of Al-based alloy nanocomposites. *Coatings* **2026**, *16*, 143. [CrossRef]
19. Rong, H.; Geng, Y.; Tao, J.; Zhou, X.; Zheng, J. Degradation of microstructure and macroscopic performance of boric acid-corroded concrete in nuclear power plants. *J. Chin. Ceram. Soc.* **2026**, *54*, 754–767. [CrossRef]

Disclaimer/Publisher's Note: The statements, opinions and data contained in all publications are solely those of the individual author(s) and contributor(s) and not of MDPI and/or the editor(s). MDPI and/or the editor(s) disclaim responsibility for any injury to people or property resulting from any ideas, methods, instructions or products referred to in the content.